Chapter 14
Acoustic Emission in Rolling Contacts

Mikhail Popov, Justus Benad, Valentin L. Popov and Markus Heß

14.1 Introduction

Technical surfaces typically have roughness ranging from the size of the system to the nanometer scale. During sliding or rolling on rough surfaces, vibration occurs that results in audible and inaudible acoustic emission. In 2006 Ford und Thompson [1] used a one-dimensional model for the analysis of the acoustic emission of a rolling wheel. This model was identical to the method of dimensionality reduction, although Ford and Thompson chose to call it two-dimensional. They compared the results obtained with the one-dimensional model with results of boundary element simulations and found very good agreement in the entire spectral range. They came to the conclusion that the 1D-model "might have an unexpectedly wide range of applicability."

The method of dimensionality reduction can be applied not only for analysis of mean values of forces but also of their fluctuations. This is confirmed by the results shown in Fig. 14.1. This figure shows the results of simulations in which a rigid indenter with random self-affine roughness (with Hurst exponents ranging from $H = 0.4$ to $H = 1$) was pressed into an elastic half-space. The three-dimensional calculations were performed with the boundary element method. 60 random surfaces were generated and the mean values as well as the standard deviation of the contact stiffness were computed for each normal force. The same calculation was performed with the equivalent one-dimensional model for 500 random realizations. The comparison of the results shows very similar behavior of the standard deviation in both the three-dimensional and one-dimensional model. Because the rolling or sliding motion continuously brings new parts of the surfaces into contact, this can be interpreted as contacts with different random realizations of the roughness. This suggests that the one-dimensional model can describe the dynamic behavior of rolling contacts.

V.L. Popov and M. Heß, *Method of Dimensionality Reduction in Contact Mechanics and Friction*, DOI 10.1007/978-3-642-53876-6_14

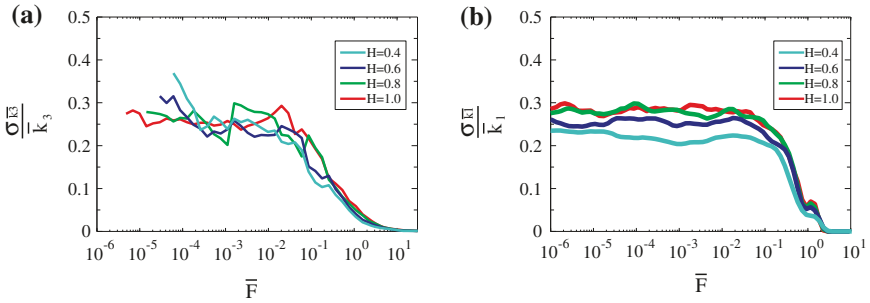

Fig. 14.1 (**a**) Relative standard deviation of the stiffness as a function of normal force for 60 realizations of three-dimensional boundary element simulations, as presented in [2]. (**b**) Relative standard deviation in the one-dimensional case, computed with 500 realizations. Data provided by R. Pohrt

In this chapter, the force fluctuations due to surface roughness of the contacting bodies will be investigated using the method of dimensionality reduction.

14.2 Acoustic Emission Resulting from the Rolling of a Wheel—An Analytical Solution

The system under consideration is a cylindrical steel wheel with a radius R and mass m that is loaded with a constant normal force F_N and is rolling on a steel rail with a velocity v_0. The rail is assumed to have the same transverse radius of curvature such that the entire problem can be reduced to the rolling of a sphere with a radius R on a half-space. The wheel and the rail both have surface roughness that can be characterized by an isotropic power spectrum. The dynamics of the wheel assembly and car structure is not considered here and is only represented through the constant normal force. Thus, we obtain our model which will be studied numerically and analytically in the following: An elastic, rough sphere rolls on a rigid, flat surface. The roughness-induced normal acceleration of the sphere is determined. This three-dimensional, dynamic contact problem is difficult to solve with traditional methods (e.g., finite elements or boundary elements) due to the extremely large computational cost. In the framework of the reduction method, however, an almost complete analytical solution is possible.

Let us consider the one-dimensional representation of the rolling wheel on a rough surface (Fig. 14.2). The form of the wheel is given by the macroscopic substitute profile

$$z = Z_0(x - \tilde{x}) \tag{14.1}$$

with

$$Z_0(x) = \frac{x^2}{R}, \tag{14.2}$$

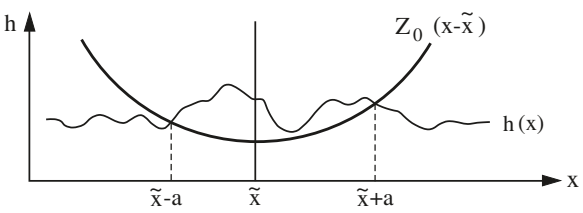

Fig. 14.2 One-dimensional representation of the rolling wheel on a rough surface

where $\tilde{x}$ is the coordinate of the wheel center. The profile of the rough surface is given by

$$z = h(x). \tag{14.3}$$

The numerical analysis of this system can proceed without additional assumptions. For the analytical solution, however, we will make some additional simplifications. First we assume that the indentation depth d is much larger than the rms value of the roughness. Under this assumption, the coordinates of the left and right boundaries of the contact depend only weakly on $\tilde{x}$ and we will assume that

$$\begin{aligned} x_1 &= \tilde{x} - a, \\ x_2 &= \tilde{x} + a, \end{aligned} \tag{14.4}$$

where a is the Hertzian contact radius for the contact of a sphere with a smooth plane. We also assume that the indentation depth remains approximately constant and experiences only small deviations from its mean value. This corresponds to a constant contact radius a. The normal force is then calculated according to the rules of the reduction method as

$$F_N(\tilde{x}) = E^* \int_{\tilde{x}-a}^{\tilde{x}+a} (h(x) - Z_0(x-\tilde{x}))\mathrm{d}x = E^* \int_{\tilde{x}-a}^{\tilde{x}+a} h(x)\mathrm{d}x - E^* \int_{\tilde{x}-a}^{\tilde{x}+a} Z_0(x-\tilde{x})\mathrm{d}x. \tag{14.5}$$

The second part of this equation does not depend on $\tilde{x}$. It follows that

$$\frac{\mathrm{d}F_N(\tilde{x})}{\mathrm{d}\tilde{x}} = E^*\big[h(\tilde{x}+a) - h(\tilde{x}-a)\big], \tag{14.6}$$

which results in

$$F_N(\tilde{x}) = E^* \int \big[h(\tilde{x}+a) - h(\tilde{x}-a)\big] d\tilde{x}. \tag{14.7}$$

Let us now assume that the rough profile is given by the customary Eq. (10.5)

$$h(x) = \sum_{q=-\pi/\Delta x}^{\pi/\Delta x} B_{1D}(q)\exp(i(qx + \phi(q))), \tag{14.8}$$

where

$$B_{1D}(q) = \sqrt{\frac{2\pi}{L} C_{1D}(q)} = \bar{B}_{1D}(-q), \tag{14.9}$$

the discretization step is given by $\Delta q = 2\pi/L$, and the random phases $\phi(\vec{q}) = -\phi(-\vec{q})$ are equally distributed on the interval $[0, 2\pi)$. It follows that

$$\begin{aligned} h(\tilde{x}+a) - h(\tilde{x}-a) &= \sum_{q=-\pi/\Delta x}^{\pi/\Delta x} B_{1D}(q)\exp(i(q\tilde{x}+\phi(q)))\left[\exp(iqa) - \exp(-iqa)\right] \\ &= \sum_{q=-\pi/\Delta x}^{\pi/\Delta x} 2iB_{1D}(q)\exp(i(q\tilde{x}+\phi(q)))\sin(qa) \end{aligned} \tag{14.10}$$

and

$$F_N(\tilde{x}) = E^* \sum_{q=-\pi/\Delta x}^{\pi/\Delta x} \frac{2}{q} B_{1D}(q)\sin(qa)\exp\left(i(q\tilde{x}+\phi(q))\right). \tag{14.11}$$

From this equation, we see immediately that the spectral density $C_{1D}(q)$ of the roughness and the spectral density $C_F(q)$ of the normal force are connected by the following relationship:

$$C_F(q) = \frac{4E^{*2}}{q^2} C_{1D}(q)\sin^2(qa). \tag{14.12}$$

In the case of a randomly self-affine rough surface with the spectral density $C_{2D}(q) = Aq^{-2H-2}$, the equivalent one-dimensional spectral density is given by the rule of Geike [Eq. (10.12)] as $C_{1D}(q) = \pi q C_{2D}(q) = \pi A q^{-2H-1}$. The spectral density of the force is then given by

$$C_F(q) \approx \frac{4E^{*2}}{q^2} A\pi q^{-2H-1}\sin^2(qa). \tag{14.13}$$

This dependence is shown for $H = 0.7$ in Fig. 14.3. Under the assumption that $qa \gg 1$, $\sin^2(qa)$ is a quickly oscillating function with the mean value $1/2$. Averaging over these oscillations gives

$$\langle C_F(q)\rangle = \frac{2E^{*2}}{q^2} C_{1D}(q). \tag{14.14}$$

This relation makes it possible to deduce the spectral density of the contact force from the spectral density of the roughness, and vice versa.

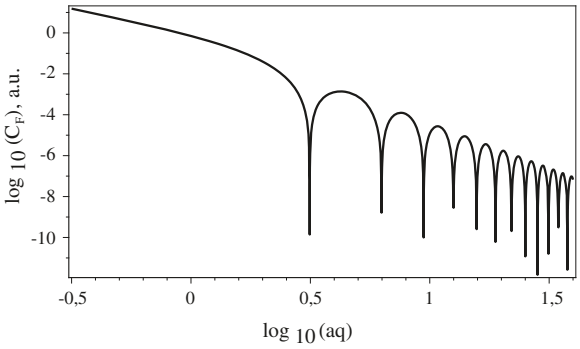

Fig. 14.3 Dependence of the power spectrum of the normal force on the wave number

14.3 Acoustic Emission Resulting from Rolling of a Wheel—A Dynamic Simulation

With the reduction method, we can easily perform full dynamic simulations of the rolling motion. In this section, we present the results of such simulations. They are also an example of the hybrid models as described in the previous chapter. The rolling of the wheel with the velocity v_0 is modelled by shifting the "spherical profile" in the positive x-direction with the velocity v_0, while the roughness profile remains stationary:

$$z(x,t) = \frac{(x - v_0 t)^2}{R} + h(x). \tag{14.15}$$

This profile is explicitly time-dependent and results in variations of the contact force F_{cont}, which in turn causes vertical motion. The equation of motion of the wheel

$$m\ddot{z}(t) = F_{cont} - F_N \tag{14.16}$$

is solved numerically, with re-computation of F_{cont} (using the reduction method) in every integration step. The time step of the dynamic simulation is set to $\Delta t = \Delta x / v_0$, so that the system moves by one spatial discretization unit during every time step. The immediate result of the dynamic simulation is the time dependence of the vertical coordinate of the wheel $z(t)$. The second derivative of the coordinate produces the normal acceleration $a(t)$. Since the acceleration is, like the roughness, a statistical quantity, we will characterize it through its spectral density, which is computed as follows:

$$A = |\mathrm{FFT}(a)|^2 \frac{\Delta t^2}{T}. \tag{14.17}$$

Here, FFT(a) denotes the fast Fourier transform of the acceleration, and T is the total simulation time.

Table 14.1 Parameters of the simulation

$E = 210\,\text{GPa}$	Elastic modulus of steel
$\nu = 1/3$	Poisson's number of steel
$R = 0.5\,\text{m}$	Radius of wheel
$M = 500\,\text{kg}$	Mass of wheel
$h_0 = 0.5\,\mu\text{m}$	Roughness

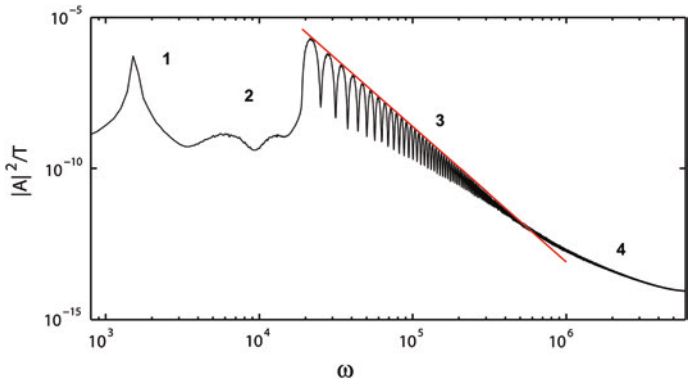

Fig. 14.4 A typical dependence of the spectral density of the acceleration on the frequency

The parameters that were used for the simulation are summarized in Table 14.1. The roughness was randomly self-affine and had the power spectrum

$$C_{1D} = const \cdot q^{-2H-1} \tag{14.18}$$

with wave numbers in the interval

$$q_{\text{min}} < |q| < q\text{max}. \tag{14.19}$$

The constant in (14.18) was chosen such that the average roughness of the profile, defined as $h = \sqrt{\langle h(x)^2 \rangle}$, was exactly equal to h_0.

The simulation was run 300 times with different realizations of the rough profiles. The averaged result of the spectral density of the acceleration as a function of frequency is shown in Fig. 14.4.

The spectrum of the acceleration can be divided in four regions:

1. In the first region there is a sharp, quickly decaying maximum.
2. Then follows a "plateau" with an oscillating substructure.
3. There is a sharp rise at the beginning of the third region, which falls linearly in double-logarithmic coordinates. This region also shows an oscillating substructure.
4. The last region with a different slope than region 3 continues to the maximum frequency $\omega_{\text{max}} = q_{\text{max}} v_0$.

The third region has an oscillating substructure with a constant period of $\Delta\omega_3$ (in the frequency domain!). The origin of this region and its substructure was already explained by the above analytical treatment. The oscillation results from the factor $\sin^2(qa)$ in (14.12), where $\Delta\omega_3 = \pi/a$. The slope (in double-logarithmic axes) in region 3 is equal to $\alpha = -2H - 3$, which follows directly from Eq. (14.13).

The other regions were not predicted by the analytical treatment; they arise due to non-linearity of the system dynamics of the contact, which was neglected for the analytical calculation. Only in the direct numerical simulation do these effects become apparent.

In the following, we discuss the physical nature of the above four regions.

1. The first peak of the spectral density coincides exactly with the resonance frequency of the wheel $\omega_{eigen} = \sqrt{2aE^*/m}$. Parameter studies show that this frequency does not depend on any of $q_{\min}$, $q_{\max}$, v_0 or H. This confirms that the peak is in fact the eigen frequency of the wheel.
2. The "plateau" after the resonance peak may or may not have a substructure, depending on the parameters.
3. Power-law region.

   The third region begins with a sharp rise in the power spectrum. It seems plausible to suppose that this rise is linked to the cutoff (i.e., the value of $q_{\min}$) in the assumed roughness spectrum. It turns out that the rise, and therefore the start of the third region, is indeed found at the frequency

$$\omega_{jump} = q_{\min} v_0, \tag{14.20}$$

   which is directly dependent on the smallest wave number in the roughness spectrum. This relationship was confirmed by variation of both the velocity and

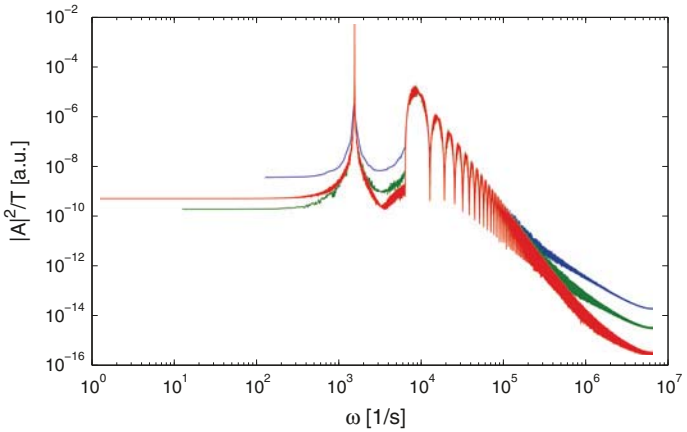

Fig. 14.5 Results of simulations with identical roughness parameters but different rolling distances, and therefore, more elements (*blue*—smallest distance, *red*—longest distance)

the cut-off wave number. At small velocities, the jump moves closer to the resonance peak, and the plateau "2" may disappear entirely.

4. "Break" in the spectral density

   The third and fourth regions are separated by a "break." The fourth region is related to the finite simulation. If the rolling of the wheel is simulated over a very long distance, the frequency of the "break" moves further to the right, and will probably disappear entirely with sufficiently long distances. This can be seen in Fig. 14.5, where the results of simulations with different rolling distances are shown. A possible explanation is that the last region is due to the spectrum of the finite "window function," which decreases very slowly at high frequencies. In any case, region 4 seems to be an artifact of the simulation that can be reduced by using more elements.

References

1. R.A.J. Ford, D.J. Thompson, Simplified contact filters in wheel/rail noise prediction. J. Sound Vibr. **293**, 807–818 (2006)
2. R. Pohrt, V.L. Popov, A.E. Filippov, Normal contact stiffness of elastic solids with fractal rough surfaces for one- and three-dimensional systems. Phys. Rev. E **86**, 026710 (2012)